

AERODYNAMIC OPTIMIZATION OF HIGH-ALTITUDE PROPELLER COMBINED WITH MACHINE LEARNING METHOD

Dichen Li^{*,1,2}, Ziyu Ge^{1,2}, Rongfeng Cui^{1,2}, Long Yang², Chuang Wei² & Wenping Song¹

1 School of Aeronautics, Northwestern Polytechnical University, Xi'an 710072, China

2 Aero Science Key Lab of High Reynolds Aerodynamic Force at High Speed, AVIC Aerodynamics Research Institute, Shenyang 110134, China

Abstract

This paper presents an optimization design for a high-altitude propeller. The machine learning method are coupled into the propeller analysis and optimization workflow to improve the calculation accuracy and efficiency. The selected E387-based propeller is from a HALE UAV, which designed to cruise at 25.9km altitude, 0.4 Mach. The propeller aerodynamic analysis is conducted by ARI_PROP, an in-house code based on Standard Strip Theory. To better solve the problem of prediction inaccuracy and complexity at high altitudes (high subsonic and low Reynolds number condition), the code employs Gaussian Progress Regression (GPR) to generate airfoil section aerodynamic performance. The GPR model can be trained by small amount of RANS CFD or experimental samples, and output accurate predictions at desired state instantly. Compared with literature and Moving Reference Frame (MRF) CFD results, ARI_PROP code shows good accuracy and automation capability. Next, the ARI_PROP code is coupled with our ARI_XunZhu optimization software, which is advantageous in high-efficiency and robustness. The software employs the Surrogate-based optimization scheme, which uses models like Kriging to establish the surrogate approximation model and guide the searching for better designs. By using the proposed overall workflow, the radial distribution of chord and pitch angle of referenced propeller that can offer maximum thrust at design point is found. The result shows that the optimized propeller's thrust increases 75.2% with efficiency set as 81%, compared to the original design.

Keywords: propeller, aerodynamic optimization, low Reynolds number, machine learning

1. General Introduction

Recently, many attention has turned towards to high-altitude long-endurance unmanned air vehicles (HALE UAV) and Martian exploration UAVs. And propellers are the most widely-used propulsion system for these aircrafts. One of the common challenges they faced is the high subsonic and low Reynolds number aerodynamics (Ma=0.4~0.9, Re=10⁴~10⁵), as both the earth near-space atmosphere and Martian atmosphere has low air density and speed of sound. Therefore, for these aircrafts with limited energy sources, it is of great necessity to study the propeller design and optimization. And the primary goal of this paper is to improve the high-altitude propeller's aerodynamic efficiency by optimization design.

Prior researches mainly focused on low-altitude propeller design and optimization, with few works dedicated for high-altitude propeller. Koch[1] studied the high-altitude propeller with ADPAC code. Kelly[2] and Young[3] analyzed a Martian rotor by both experiment and calculation, finding that the propeller tip sections need to be carefully designed. Recently, some studies[4][5] devoted to designing unconventional section airfoil, such as flat/cambered plate and triangular airfoil, for propeller at ultra-low Re=10³~10⁴. In summary, the majority of current works still use the traditional propeller design and optimization method, which is developed particularly for low-altitude propeller. By doing so, the high subsonic and low Reynolds number effect of high-altitude propeller is mistakenly neglected, and the results reliability is questionable.

This paper focuses on improving aerodynamic performance of high-altitude propeller at cruise state,

which is a typical high subsonic and low Reynolds number condition. And a new set of approaches especially for this unique problem is proposed. Particularly, with the recent rapid development of machine learning techniques, these ideas are coupled into our approaches for propeller calculation and surrogate-model-based optimization. Finally, the result analysis and conclusions are presented.

2. Optimization Design Methodology

The optimization design method used in this paper is shown in Figure 1. It mainly consists of two parts, the ARI_PROP propeller analysis code and ARI_XunZhu optimization software. Both parts are our self-developed in-house software written in FORTRAN programming language. The ARI_PROP is a Standard-Strip-Theory-based fast analysis tool. It is developed particularly for high-altitude propeller and can give accurate results in several minutes. The ARI_XunZhu software is our general optimization platform. It is capable of solving single/multi-objective optimization problem under multi-constraints, and has been applied on many high-precision CFD aerodynamic optimization cases, as well as aerodynamic/structural/stealth multi-disciplinary optimization design projects. It contains surrogate-based optimization scheme, which is advantageous in high-efficiency and robustness

In present work, two parts are coupled together. The optimization workflow will repeatedly call the propeller analysis code to fill the Data container with calculated results. The contained data will be used to build the surrogate model for optimal-seeking process. On the other hand, the iterative calculation procedure of ARI_PROP code will repeatedly call the C_L and C_D of blade element airfoils. These aerodynamic characteristics are modelled and predicted by Gaussian Process Regression method, which employs sampled numerical and experimental data as inputs, and outputs result of desired state almost instantly.

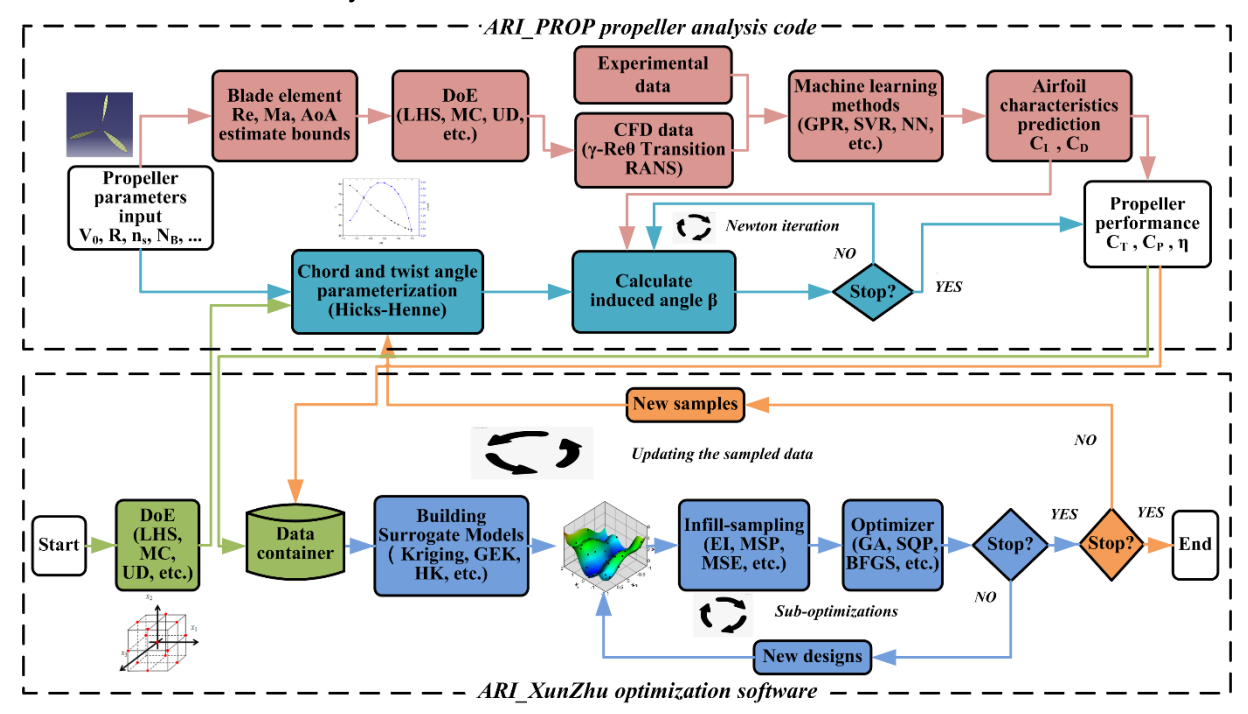


Figure 1. Overall flow diagram

2.1 Propeller Aerodynamic Analysis

The Standard Strip Theory is the formulation basis for propeller analysis. It treats blade as a set of divided blade elements, and the blade element is regarded as a two dimensional airfoil. The local flow schematic of the airfoil is presented in Figure 2.

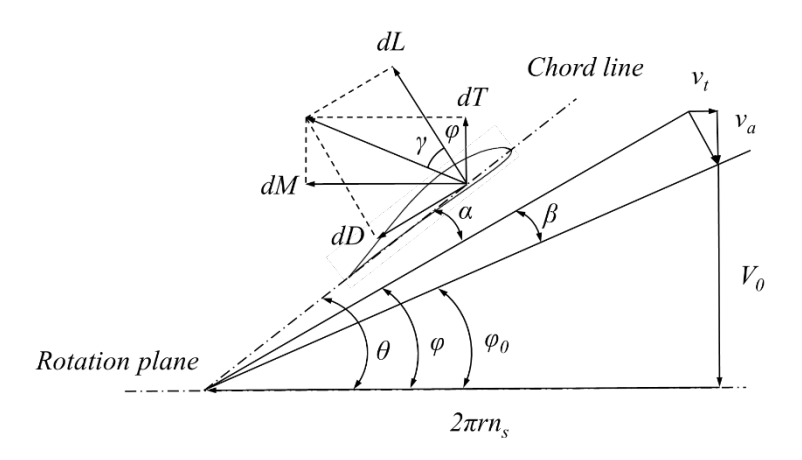


Figure 2. Schematic of blade element forces

The detailed formulation will not be elaborated here for simplicity. Basically, by correlating the momentum theory and blade element force analysis, the induced angle β can be calculated by below equation using Newton iteration method.

$$C_L \frac{N_B b}{2\pi r n_s} = \frac{4\sin(\phi_0 + \beta)\tan\beta}{1 - \tan\gamma\tan\beta} \tag{1}$$

And the increment thrust and torque of each blade element can be determined by

$$dT = \frac{1}{2} \rho V_0^2 \frac{C_L b (1+a)^2}{\sin^2 \phi \cos \gamma} \cos(\phi + \gamma) dr$$
 (2)

$$dM = \frac{1}{2} \rho V_0^2 \frac{C_L b (1+a)^2}{\sin^2 \phi \cos \gamma} r \sin(\phi + \gamma) dr$$
 (3)

Here, the blade element's radial position is r, local chord is b, V_0 is the forward speed of the propeller, θ is the pitch angle, φ is the actual flow angle, ratio $\gamma = \arctan(C_D / C_L)$, axial induction factor $a = v_a / V_0$, N_B is the number of blades, n_s is the rotational speed. The current formulations also take into account the hub and tip loss. These corrections are given by Prandtl and Glauert[6] for momentum equations during each iteration. The radial movement of the flow is also considered. The 3D Flow Equilibrium Model of Saravanamuttoo[7] is applied. By integrating equation (2) and equation (3) along the blade radius, the thrust and power coefficients are calculated as

$$C_T = \frac{T}{\rho n_s D^4} \tag{4}$$

$$C_P = \frac{M2\pi}{\rho n_s^2 D^5} \tag{5}$$

The advance ratio λ and propeller efficiency η are

$$\lambda = \frac{V_0}{n_c D} \tag{6}$$

$$\eta = \lambda \frac{C_T}{C_P} \tag{7}$$

Usually, there are two ways to obtain the aerodynamic data of airfoil section in common propeller fast analysis software: (a) Direct calculation of code like panel-method-based XFOIL; (b) Imported datasets. The first one is the most widely used way. However, it does not work for high-altitude propeller. Because the element airfoils work at high subsonic and low Reynolds number condition, this often leads to convergence failure for XFOIL calculation. The second way is a more accurate option. But traditional practice also does not work well for high-altitude propeller. Traditionally, small amount of data either from experiment or numerical simulation are directly used or by simple linear

interpolation. This is because the airfoil sections of ordinary propellers work at high Reynolds number condition, and the aerodynamic characteristics nearly does not change at subsonic speeds. Thus, one only needs to search the published experimental reports or conduct numerical simulations to get several typical data, then it would be enough.

Contrarily, the high-altitude propeller should require large amount of accurate data. Because, as mentioned before, the airfoil section work at high subsonic and low Reynolds number condition. Figure 3 shows the reference propeller designed for near-space aircraft[1]. The propeller uses E387 airfoil as blade element, and is designed to cruise at 25.9km altitude, 0.4 Mach. In this environment, as show in Figure 3, the airfoil section from hub to tip works at Ma=0.41~0.79, Re=4.8×10⁴~1.88×10⁵. Under this unique flow regime, the aerodynamic characteristics is very sensitive to flow conditions. In other words, from propeller hub to tip, a slight change of Re or Ma will lead to big differences of C_L and C_D [8][9]. Therefore, large amount of wind tunnel experimental or numerical simulation data that covers the whole Re, Ma, AoA range is required, which makes the practice very expensive and time-consuming.

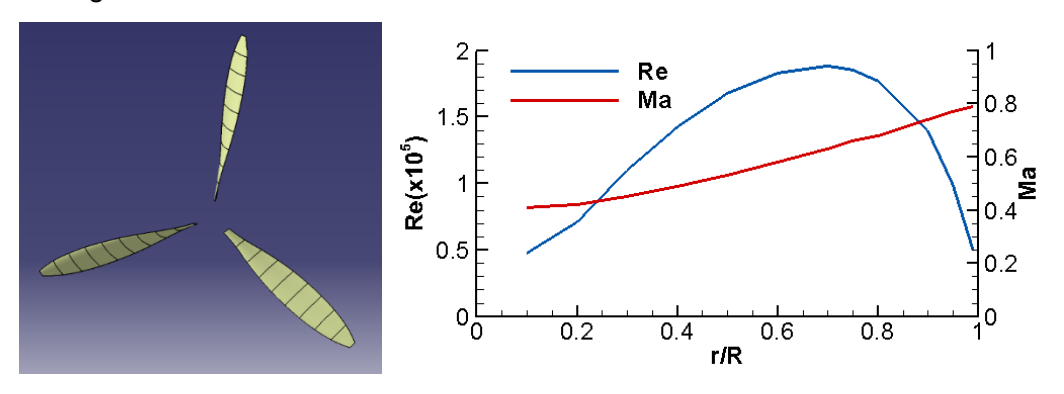


Figure 3. Reference propeller and its radial distribution of Re and Ma

Presently, with the rapid development of machine learning, the technique has been applied on various fields including aerodynamic modelling. It establishes an approximate relationship between input flow conditions and output aerodynamic forces, based on a few set of trusted data. And use this relationship model to predict forces at desired conditions, to reduce or partially replace CFD and wind tunnel experiments. Here, as the Gaussian Process Regression (GPR) method[10] shows excellent performance of prediction reliability and robustness[11], it is selected from many machine learning techniques in this work. The Python Scikit-learn toolbox is used here. The aerodynamic characteristics C_L and C_D are the model prediction objects. The model input parameters are Re, Ma and AOA, which should cover the range of Ma=0.4~0.8, Re=4×10⁴~2×10⁵, AOA=-4° ~12°. The Latin Hypercube Sampling (LHS) method[12] is used in the Design of Experiment (DoE) process to randomly sample the inputs, 300 samples are used to train the approximation model, and the other 239 samples are used to analyze the errors of the model. The CFD method is used to calculate the samples' response. Specifically, Transition SST (γ-Re_θ) RANS is used for E387 airfoil section aerodynamic forces simulation. The details of CFD settings and validation can be found in our previous work[9]. The calculated results of 300 LHS samples are shown in Figure 4, It again demonstrates that the C_L and C_D are very sensitive to Ma, Re and AoA within studied realm

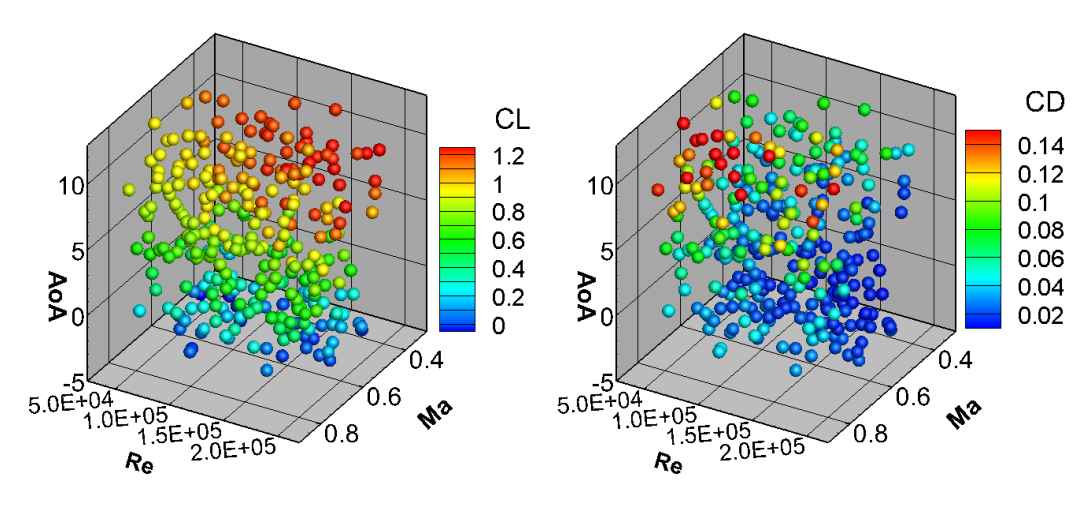


Figure 4. Distribution and values of DoE samples

Here, the residual normality test is conducted to verify the model's rationality. Figure 5 shows the residual histogram of C_L and C_D of 239 predicted results. It can be seen that the results well satisfy the normal distribution, which indicating that the prediction residual is generated completely randomly. The modelling method causes no bias to prediction results and is therefore rational.

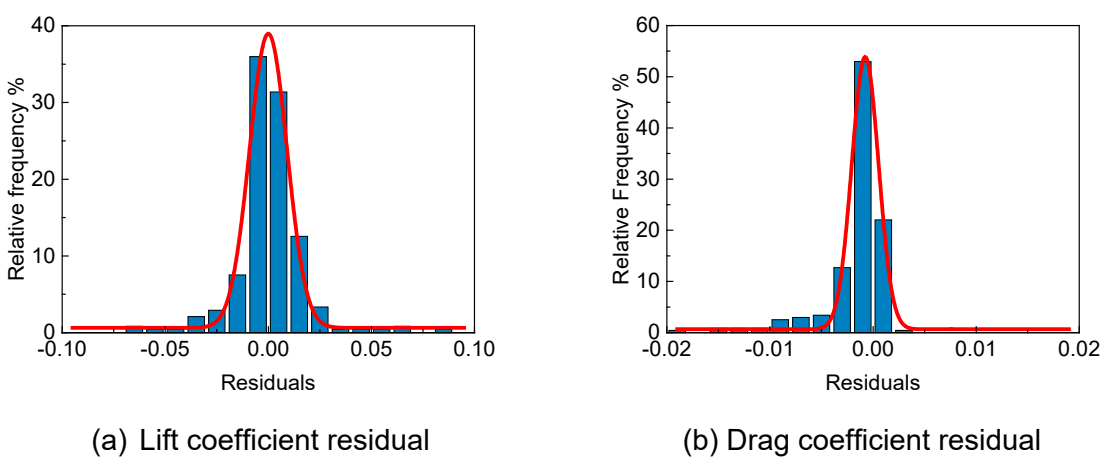


Figure 5. Residual histogram of GPR model ratioanlity verification Moreover, the Mean Absolute Percentage Error (MAPE) is used to evaluate the accuracy of model prediction results.

$$MAPE = \frac{1}{N} \sum_{i=1}^{N} \left| \frac{y_{pre} - y_{cal}}{y_{cal}} \right|$$
 (8)

where y_{pre} is GPR model predicted value, y_{cal} is RANS CFD value, N=239 is the number of predicted results. The MAPE value ranges from 0~100%, the smaller the value, the more accurate the prediction. The MAPE of C_L and C_D are 4.63% and 3.06%, respectively. It indicates that the GPR model has good non-linear fitting ability with relatively small amount of training samples.

To further demonstrate the prediction effect of present model, the lift and drag coefficients at Ma=0.4, Re=5×10⁴, AOA=-5° ~15° and Ma=0.63, Re=1×10⁵, AOA=-5° ~15° are compared with RANS CFD results. Note that in Figure 6, some marginal AOAs predicted here are out of the range of training samples, which could happen when calculating the propeller off-design performances. However, the predictions still well match CFD results over the whole range, which exhibits good model prediction accuracy.

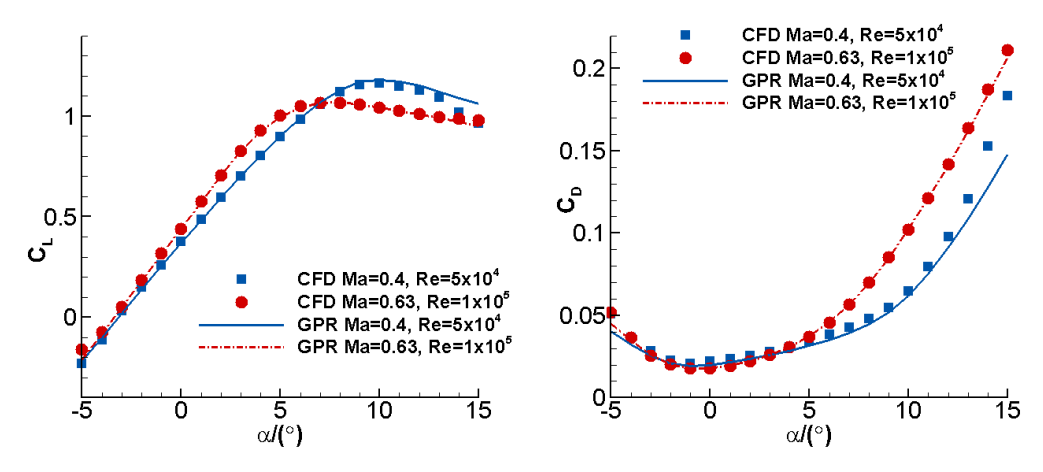


Figure 6. Comparison of GPR prediction and CFD results

To demonstrate the validity of the ARI_PROP code, the performance of aforementioned reference propeller is calculated for a wide range of advance ratio. Due to the lack of experimental data, the results are compared with other strip theory analysis[1] and Moving Reference Frame (MRF) CFD simulation. For MRF CFD, the computational domain and grid are shown in Figure 7. The domain consists of two parts, the inner rotating zone and the outer stationary zone. The total grid contains 23.4 million cells. The detailed introduction of case setup and grid information can be found in our previous work[9]. The JBLADE[13] software is also used for comparison. The software couples the Blade Element Method formulation and XFOIL for propeller design and analysis. However, unfortunately, the XFOIL code fails to give converged results at high subsonic and low Reynolds number condition. Therefore, the airfoil aerodynamic dataset at different radial stations has to be calculated by RANS CFD firstly and then imported into JBLADE, which is a manual and cumbersome process.

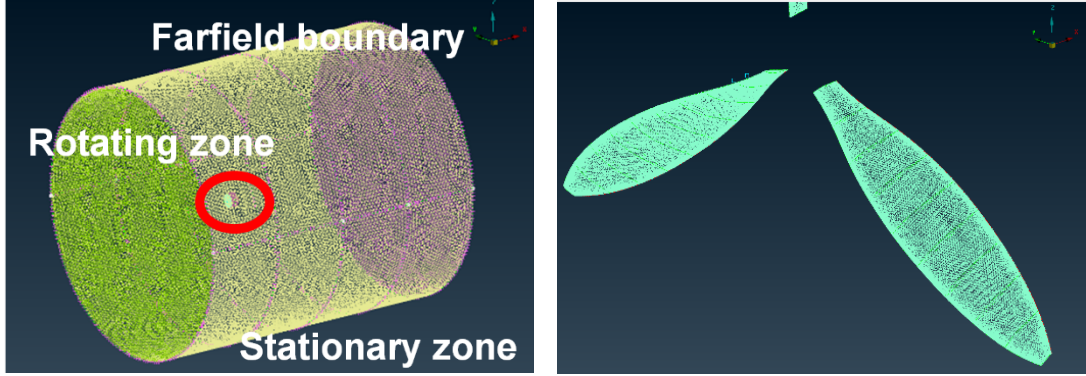


Figure 7. MRF CFD grid of propeller

The thrust coefficient C_T , power coefficient C_P and efficiency η of the propeller are shown in Figure 8. As no published experimental data exists, the MRF CFD results is considered to be a reliable reference. It can be seen that all the fast analysis results well match the MRF CFD result. This is because the strip theory of literature uses validated ADPAC code to calculate the airfoil section performance, and the JBLADE also uses our imported airfoil section performance by RANS CFD. Even though, compared with others, our ARI_PROP code exhibits a better agreement with MRF CFD result over the whole range of advance ratio. This is largely because of the airfoil section GPR model trained by accurate RANS CFD results. Besides, our code can be executed fully automatically and requires no data-import manual operations, which is crucial for optimization process. Hence, the ARI_PROP code prove its reliability and will be used in the following optimization study.

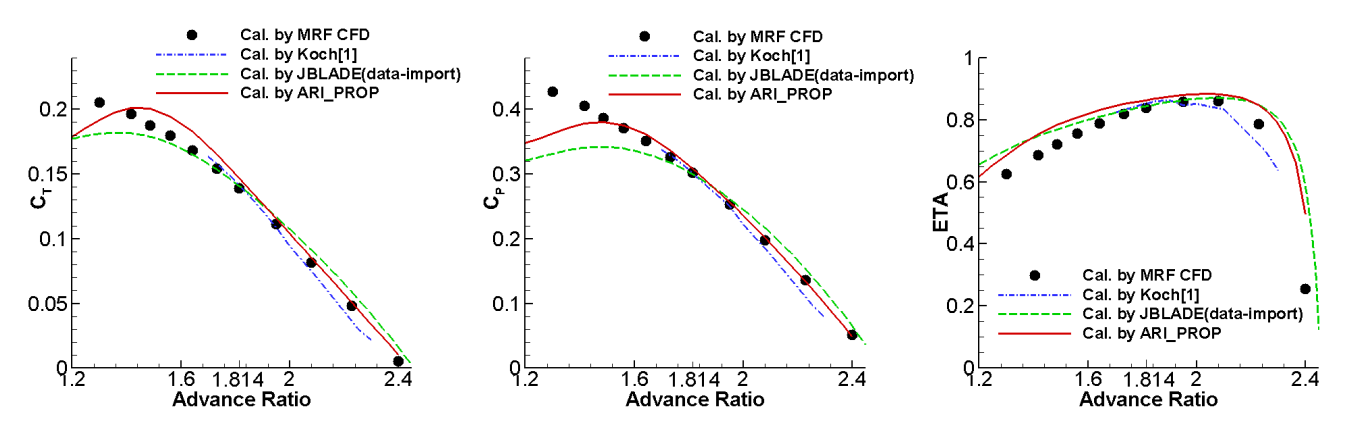


Figure 8. Propeller performance comparison

2.2 Propeller Optimization Design

The design parameters of propeller usually include diameter, rotation speed, blade number, pitch angle distribution, local chord distribution and sectional airfoil shape. Here, the pitch angle distribution $\theta(r)$ and local chord distribution b(r) are selected. For the purpose of reducing design variables, the parameterization method is used to mathematically describe $\theta(r)$ and b(r). Here, we choose the improved Hicks-Henne method, which uses original geometry and linear superposition of disturbance shape functions to describe deformed geometries.

$$\theta(r) = \theta_0(r) + \sum_{k=1}^{N} p_k f_k(r)$$

$$b(r) = b_0(r) + \sum_{k=1}^{N} q_k f_k(r)$$
(9)

Here, $\theta_0(r)$ and $b_0(r)$ are original distributions in the form of discrete points, p_k and q_k are the coefficients to control deformation, N is the number of coefficients, $f_k(r)$ is Hicks-Henne function as below,

$$f_k(r) = \begin{cases} r^{0.25} (1 - r)e^{-20r}, k = 1\\ \sin^3(\pi r^{e(k)}), & k > 1 \end{cases}$$
 (10)

Where $e(k) = \lg 0.5 / \lg r_k$, $0 \le r_k \le R$ and r_k is the set points between blade hub and tip. The coefficients of disturbance shape function are used as design variables, and the optimal design shape can thus be determined by original shape and design variables. Here, the $\theta(r)$ and b(r) at the hub and tip are fixed. And there are eight variables to be optimized, four variables for $\theta(r)$, which value from -15.0 to 15.0, and four other variables for b(r), which value from -0.2 to 0.2.

In optimization process, the thrust coefficient at design point λ =1.814 is considered as optimization object. The aerodynamic efficiency is set to higher than 81% as that of the maximum thrust point. The optimization problem is described as follows:

Objective:
$$max(C_T)$$

 $s.t.: \eta \ge 81\%$ (11)

The optimization is based on the ARI_XunZhu[14] optimization software. The design of experiment (DoE) process uses the Latin Hypercube Sampling (LHS) method, the Kriging model is employed for establishing surrogate model, the EI and MSP mixed sample-adding method is adopted. Genetic algorithm is used to optimize the surrogate model, the maximum evolution is 200 generations, the crossover probability is 0.9, and the mutation probability is 0.05. The optimization starts with 60 initial samples, and reaches convergence of optimization criteria after about 400 evaluations, as shown in Figure 9.

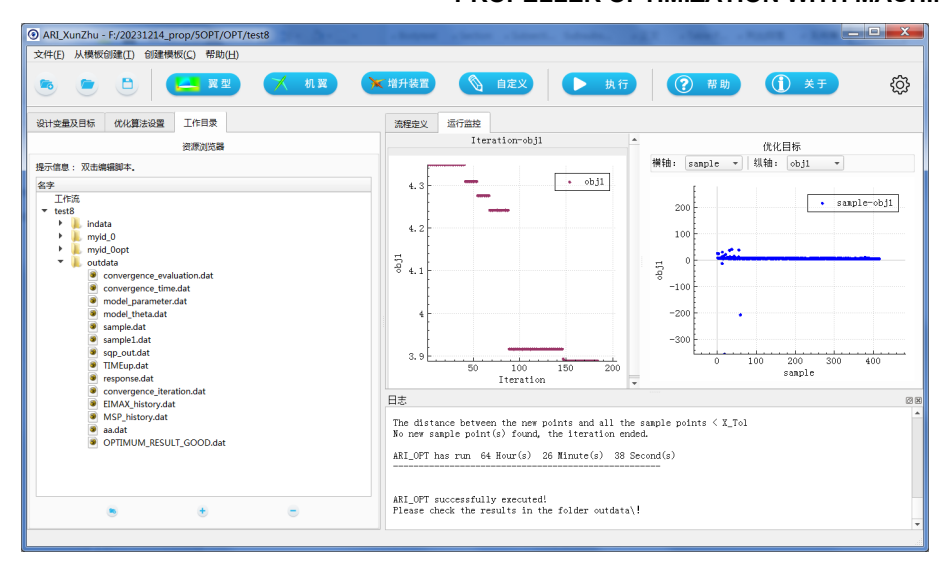


Figure 9. ARI XunZhu optimization software

Figure 10 shows the comparison of optimized propeller geometry with original. Significant changes can be clearly witnessed. The optimized airfoil section chord distribution is greatly increased over the whole span, with maximum increment 56.35% at r/R=0.7. The pitch angle distribution is also increased, mainly around r/R=0.75 which contribute the main thrust.

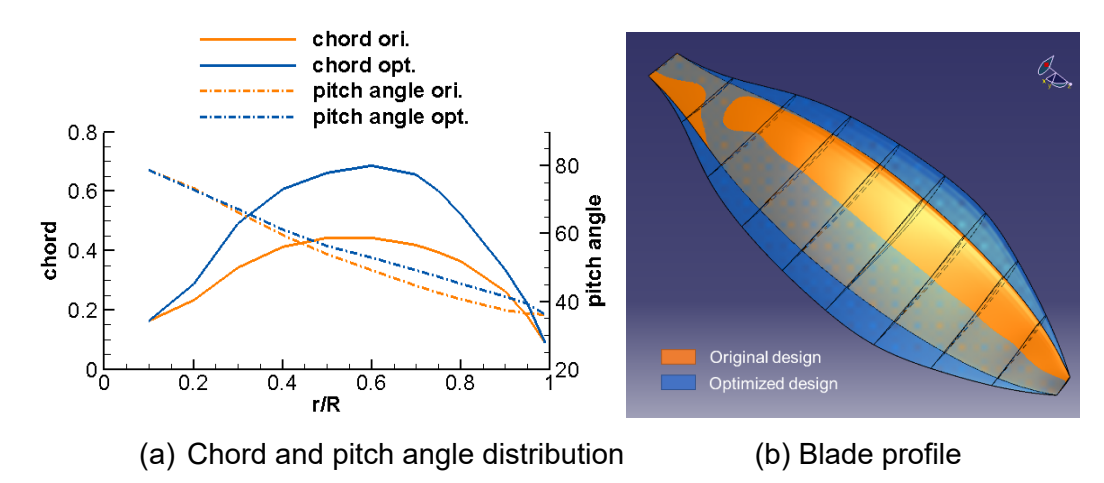


Figure 10. Comparison of propeller geometries

The aerodynamic performances of optimized propeller and original one are compared in Table 1 and Figure 11. As shown in the table, the efficiency of optimized propeller well satisfies the constraint $\eta \ge 81\%$. The optimized trust is dramatically increased by 75.2%. The MRF CFD is also conducted for optimized propeller, and the results confirmed the optimization. Figure 11 further demonstrate the pressure distribution on the blade and turbulence kinetic energy iso-surface. More flow separation for the optimized can be seen, which means more thrust is obtained at a cost of less efficiency.

Table 1. Propeller performance comparison

	Method	Efficiency %	C_T	ΔC_T
Original design	ARI_PROP	86.31	0.1468	1
	MRF CFD	83.72	0.1393	1
Optimized design	ARI_PROP	81.00	0.2572	+75.2%
	MRF CFD	78.52	0.2300	+65.1%

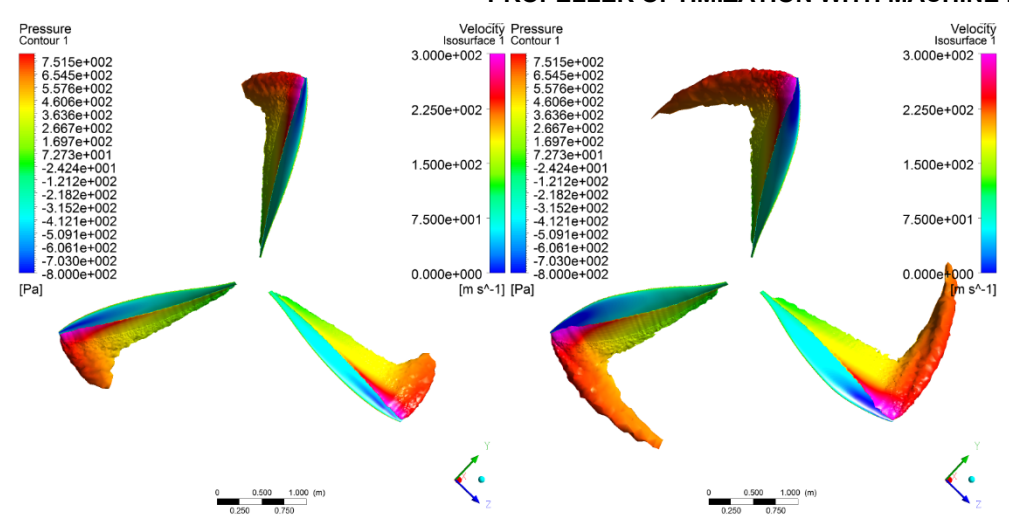


Figure 11. Comparison of propeller MRF CFD result. Left: original. Right: optimized (Turbulence kinetic energy=55J/kg, Contour color: Velocity).

3. Conclusion

A new set of optimization approaches has been proposed particularly for high-altitude propeller. The approaches combine the self-developed ARI_PROP propeller analysis code and ARI_XunZhu optimization software. By using machine learning techniques, the unique optimization problem regarding to high-altitude propeller can be well solved. The validity and accuracy of the new approaches are demonstrated by optimization case of reference propeller. Significant improvement of propeller thrust 75.2% is achieved by the optimal design, with efficiency set as 81% at design point, compared to the original design.

4. Contact Author Email Address

Dichen Li: lidichen11@163.com

5. Copyright Statement

The authors confirm that they, and/or their company or organization, hold copyright on all of the original material included in this paper. The authors also confirm that they have obtained permission, from the copyright holder of any third party material included in this paper, to publish it as part of their paper. The authors confirm that they give permission, or have obtained permission from the copyright holder of this paper, for the publication and distribution of this paper as part of the ICAS proceedings or as individual off-prints from the proceedings.

References

- [1] Koch L D. Design and performance calculations of propeller for very high-altitude flight. Case Western Reserve University, 1998.
- [2] Corfeld K, Strawn R, Long L. Computational analysis of a prototype Martian rotorcraft experiment. *20th AIAA applied Aerodynamics Conference*, St. Louis, Missouri, pp 2815, 24-26 June 2002.
- [3] Young L, Aiken E W, Derby M R, et al. Experimental investigation and demonstration of rotary-wing technologies for flight in the atmosphere of Mars. *58th Annual Forum of the American Helicopter Society*, Montreal, Canada, 58(1): 268-284, June 11-13, 2002.
- [4] Yang H, Agarwal R K. CFD simulations of a triangular airfoil for Martian atmosphere in low-Reynolds number compressible flow. *AIAA AVIATION Forum*, Dallas, Texas, pp 2923, 17-21 June 2019.
- [5] Koning W J, Romander E A, Johnson W. Optimization of low Reynolds number airfoils for Martian rotor applications using an evolutionary algorithm. *AIAA SciTech Forum*, Orlando, FL, pp 0084, 6-10 January 2020.
- [6] Glauert H. Airplane Propellers Aerodynamic Theory Volume IV edited by William Frederick Durand. pp 169-269. 1963.
- [7] Saravanamuttoo, H., Rogers, G. and Cohen, H. Gas Turbine Theory. Pearson education, 2001.

- [8] García-Gutiérrez A, Gonzalo J, Domínguez D, et al. Aerodynamic optimization of propellers for high altitude pseudo-satellites. *Aerospace Science and Technology*, 96: 105562, 2020.
- [9] Li D, Yang L, Wei C. High subsonic and low Reynolds number airfoil optimization of high-altitude propeller. *Journal of Physics: Conference Series*, 2336(1): 012017, 2022.
- [10]Williams C K I, Rasmussen C E. Gaussian processes for machine learning. Cambridge, MA: MIT press, 2006.
- [11]Çetiner A E, Yagiz B, Guzel G, et al. CFD based response surface modeling with an application in missile aerodynamics. *34th AIAA Applied Aerodynamics Conference*, pp 4336, 2016.
- [12]Mackay D. Finding fugacity feasible. Environmental Science & Technology, 13(10): 1218-1223, 1979.
- [13]Silvestre M A, Morgado J P, Pascoa J. JBLADE: a propeller design and analysis code. *International Powered Lift Conference*, Los Angeles, CA, pp 4220, 2013.
- [14]Wei C, Yang L, Li C P, et al. Research progress and application of ARI_OPT software for aerodynamic shape optimization. *Acta Aeronautica et Astronautica Sinica*, 41(5): 623370, 2020.